

## **Defects in TiO<sub>2</sub> films on p<sup>+</sup>-Si studied by positron annihilation spectroscopy**

P. G. Coleman<sup>a,\*</sup>, C.J. Edwardson<sup>a</sup>, Anbang Zhang<sup>b</sup>, Xiangyang Ma<sup>b</sup>,  
Xiaodong Pi<sup>b</sup>, Deren Yang<sup>b</sup>

<sup>a</sup> *Department of Physics, University of Bath, Bath BA2 7AY, United Kingdom*

<sup>b</sup> *State Key Laboratory of Silicon Materials and Department of Materials Science and Engineering, Zhejiang University, Hangzhou 310027, People's Republic of China*

### **ABSTRACT**

Variable-energy positron annihilation spectroscopy has been applied to the study of defects in TiO<sub>2</sub>/p<sup>+</sup>-Si structures, in the as-grown state and after annealing in vacuum and in hydrogen, to investigate whether annealing (and film thickness) resulted in an increase of vacancy-type defects in the oxide films. It was found that the concentration of such defects remained unchanged after vacuum annealing for all films studied, but after H<sub>2</sub> annealing more than doubled for 150 nm-thick films, and increased by an order of magnitude for 100nm-thick films. The nature of the vacancies was examined further by measuring high-precision annihilation lines and comparing them with a reference Si spectrum. The changes observed in the ratio spectra associated with oxygen electrons suggest that the defects are oxygen vacancies, which have been shown to enhance electroluminescence from TiO<sub>2</sub>/p<sup>+</sup>-Si heterostructure-based devices.

---

\*Corresponding author. Tel: +44 1225 383370.

*E-mail address:* p.g.coleman@bath.ac.uk (P.G. Coleman).

## 1. Introduction

Much attention has been focused on titanium dioxide ( $\text{TiO}_2$ ) in recent years because of its optical and electronic properties [eg 1,2].

Electro-luminescence (EL) is a potentially important tool in the development of silicon-based opto-electronics. Zhang et al. [3] demonstrated for the first time EL from  $\text{TiO}_2/\text{p}^+\text{Si}$  heterostructures, attributing the EL to recombination between electrons at  $V_{\text{O}}$  (oxygen vacancy) levels and holes in the valence band. Consequently Zhang et al. [4] found a correlation between EL from these heterostructures and the concentration of  $V_{\text{O}}$  in the oxide film produced by argon plasma treatment.

As room-temperature luminescence from  $\text{TiO}_2$  is associated with defect-related light-emitting centers, it is to be expected that positron annihilation spectroscopy (PAS) – a technique with exceptional sensitivity to open-volume point defects – should be applied to investigate the defect structure of  $\text{TiO}_2$ . Information on  $V_{\text{O}}$  in plasma-treated  $\text{TiO}_2/\text{p}^+\text{Si}$  samples was gained by the application of the variable-energy form of PAS (VEPAS) [4].

In VEPAS positrons of controllable energy (with a spread of  $\sim 1\text{eV}$ ) are implanted into samples with mean energies of between 0.1 and 30 keV, corresponding to mean depths from the surface to several  $\mu\text{m}$ . Measurement and analysis of annihilation gamma ray energy spectra yields information on atomic-scale structure via the measurement of Doppler broadening associated with the mean electron momentum at the annihilation sites, which is typically expressed by the single-number parameter  $S$  [5]. The peaked depth profile of the implanted positrons has a full-width-at-half-maximum approximately equal to the mean depth, so that the depth resolution degrades at depths greater than a few  $10^2$  nm and the standard fitting code VEPFIT [6] is required to obtain semi-quantitative information on defect depths and concentrations. Nevertheless, VEPAS is well suited to the study of films of  $\sim 10^2$  nm

thickness, as in the present case. It has, for example, been used to investigate the defect structure of high- $k$  TiO<sub>2</sub> films on SiO<sub>2</sub>/SiC substrates. [7-9]

The present work was motivated by preliminary observations of EL enhancement by annealing TiO<sub>2</sub>/p<sup>+</sup>Si structures in vacuum or hydrogen ambient, with EL intensity also increasing with oxide film thickness, and to investigate (using VEPAS) whether these observations were also related to V<sub>O</sub> concentration.

## 2. Experimental procedure

TiO<sub>2</sub>/p<sup>+</sup>-Si heterostructures were prepared by the thermal oxidation (500°C, 2h) of sputtered Ti films on heavily boron-doped silicon (p<sup>+</sup>-Si) substrates. The TiO<sub>2</sub> film thicknesses were 100, 150 and 220 nm; there was a thin SiO<sub>2</sub> layer between film and substrate. The samples were annealed in vacuum or in hydrogen at 500°C for 1h. The pressures for the annealing in vacuum and in hydrogen were  $8 \times 10^{-3}$  and 2 Pa, respectively, and the samples were cooled in the same ambients at 0.7 °C/min. until the temperature dropped to below 100°C.

Examination of the 100 and 220 nm-thick films after H<sub>2</sub> annealing by scanning electron microscopy (SEM) showed no discernible difference in microstructure between the samples. Structural characterization of similar films was reported in ref.[4] but, as standard methods were found to be insensitive to vacancy point defects, the present study focused on the application of VEPAS.

The samples were investigated by VEPAS in the as-grown state and after annealing in vacuum and in hydrogen. The positron parameter  $S$  was measured as a function of incident positron energy  $E$  from 0.25 to 30keV, and annihilation lineshapes were recorded for samples 1-4 and 7 at 1.5/2.0 keV, and sample 1 at 2.5 keV.  $S$  was also measured for a sample of bulk single-crystal TiO<sub>2</sub>. The data were all normalized to the parameter values for bulk Si. As no

extra information was gleaned from measurement of other positron parameters (e.g.,  $W$  - see Ref. 5), this report will focus only on  $S$ .

Annihilation lineshapes were recorded for a number of the samples 1-4 at  $E$  chosen to correspond to depths of interest (see later). As the detailed shape of the annihilation line (or the photopeak centered at  $mc^2 - 511$  keV - generated by the high-resolution Ge gamma detector) is influenced in its wings by annihilations with bound atomic electrons, the ratio of such spectra to a reference spectrum such as that for effectively defect-free silicon can provide information on the chemical nature of the environment in which the positrons are annihilated. [10]

### 3. Results

Fig. 1 shows a typical  $S(E)$  plot for a 100 nm film.  $S$  falls from the surface value (at  $E \sim 0$ ) towards the value characteristic of the oxide film. Because the film thickness is comparable to the spread of the positron implantation profile, and positrons can additionally diffuse after thermalization, the measured minimum value of  $S$  does not equal that characteristic of the oxide film (that would only be recorded if all the implanted positrons were annihilated in the film). The film  $S$  is extracted using the code VEPFIT [6].  $S$  then rises again towards the substrate value (here unity) as an increasing fraction of the implanted positrons reach depths so far distant from the film that a negligible fraction are able to diffuse back to it, and instead are annihilated in the silicon.

The nature of the increase to the substrate  $S$  value is evident in the raw data; the rapid increase seen in the current data indicates that any positron implanted into the silicon substrate is annihilated with an  $S$  parameter equal or approximately equal to that of silicon – i.e., unity. The back diffusion of positrons to the low- $S$  film region is thus prevented by a

significant electric field (similar to that existing at the surface of  $p^+$ -Si as a result of band bending [11]), or by virtue of efficient interface trapping in large open volumes whose  $S$  value is unity or above, or a mixture of the two. For comparison in Fig. 1 are data for a similar 100 nm-thick film formed on the surface of a different silicon substrate. In contrast, data fitting for this second sample with VEPFIT shows that the positron diffusion back to the low- $S$  film region is hardly affected by the above-mentioned factors, indicating that the dopant concentration is lower and/or there are few large trapping sites at the interface. However, for the purposes of this study, the exact cause of the rapid rise towards unity is not important, as it is the state of the  $\text{TiO}_2$  film and the oxide-substrate interface which are of interest.

Fig. 2 shows raw data for 100 and 150nm  $\text{TiO}_2/p^+$ -Si films, as-grown and after annealing at 500°C in vacuum and in hydrogen. The data were reproducible and the plots shown are the average of many individual measurements. The top axis shows the estimated mean positron implantation depths, taking account of the different densities of the films and substrate (4 and  $2.32 \text{ g cm}^{-3}$ , respectively); these are for guidance only, as the final data are influenced both by the spread of the positron implantation depth profile and post-implantation diffusion. All data were fitted using VEPFIT [6], which is especially useful for layered structures and which assigns annihilation parameters and effective positron diffusion lengths to each layer after assuming a positron implantation profile and solving the diffusion equation; interface traps and electric fields can be incorporated into the fits.

High-precision annihilation line spectra, containing  $\sim 2 \times 10^8$  counts, were measured for the 100nm-thick oxide sample for  $E = 1.5 \text{ keV}$  – i.e., at the minimum in the  $S(E)$  data of Fig.2, for the as-grown film and after annealing in hydrogen at 500°C. Additionally, a reference spectrum for defect-free silicon was measured. The spectra were normalized to the same area or total counts. The ratios of the sample spectra to that for silicon are shown in Fig. 3. The

peaks are centered at a gamma energy  $\sim 514.6$  keV, close to that previously assigned to oxygen electrons (see, e.g., Refs. 10,12).

#### 4. Data analysis and discussion

Data for all samples could only be fit by assuming that all positrons entering the Si substrate are annihilated in the substrate – ie, they do not diffuse out of it once implanted, or they diffuse to  $\text{TiO}_2/\text{SiO}_2/\text{Si}$  interface traps whose characteristic  $S$  value is  $\geq 1$ , as described above. All the data were consequently fit with zero effective diffusion length in the substrate. Although satisfactory fits could be obtained by assuming that positrons diffusing in the film to the  $\text{SiO}_2$  interface are annihilated with a high  $S$  – similar to that characteristic of large vacancy clusters in Si (ie  $\sim 1.13$ ) – this is seen as much less likely, as (a) the only difference between samples whose data are shown in Fig. 2 is the dopant level in the substrate, and (b) large defects in  $\text{SiO}_2$  are not expected to have high  $S$  values. Electric fields in the film or interface regions could not fit the data.

Film  $S$  parameters given by VEPFIT are shown in Fig. 4. Statistical errors on the values are negligible in the numbers as shown, but fitting uncertainties are relatively large. The film  $S$  value varies if small electric fields assigned to the film, with film thickness, and with fitted positron diffusion lengths. These variations arise because the films are thin and because the raw value of  $S$  never reaches the ‘actual’ bulk film value, but rather exhibits a minimum. To account for all of these uncertainties, a systematic error bar of  $\pm .005$  is attached to each of the values shown in Fig. 4.

All the  $S$  values for the as-grown and vacuum-annealed samples overlap within uncertainties for each film, and so averages have been taken.

Fig. 4 shows that there is generally an increase in film  $S$  after annealing in  $H_2$  (but not measurably after vacuum annealing), the increase being greatest for the thinnest film, and that there is an increase with film thickness for the as-grown and vacuum-annealed samples, but not measurably in the  $H_2$ -annealed samples.

The decrease in the oxygen peak intensity as the film is annealed, an example of which is shown in Fig. 3, is consistent with the observed increase in film  $S$  for the  $H_2$ -annealed sample (there is little change in the spectrum ratios for the as-grown and vac-annealed samples), confirming that the increase in  $S$  is associated with a decreasing sensitivity to O electrons.

This observation could be explained by the passivation of Ti vacancies,  $V_{Ti}$ , by H, with a resultant decrease in positron exposure to O electrons – positrons are expected to be trapped by  $V_{Ti}$  but not by the positively-charged  $V_O$ . However,  $V_O$ , are expected to be present in much higher concentrations than  $V_{Ti}$  [13], the latter normally being produced by prolonged oxidation. Additionally, the passivation of  $V_{Ti}$  would mean that the films would appear to the positrons to be of higher quality, and the measured  $S$  would thus decrease towards the value we previously measured for bulk  $TiO_2$ , 0.8285. Therefore, the present observation is much more likely to reflect an increase in  $V_O$  concentration in the film after annealing in  $H_2$ . Similar increases have been seen in a number of previous studies – for example in  $TiO_2$  nanowires after  $H_2$  treatment between 200 and 500°C [14] and in Cr-doped  $TiO_2$  films [15].

While annealing in vacuo and in  $H_2$  have both previously been shown to lead to the creation of  $V_O$ , it is perhaps not surprising that the latter is a more efficient process. The formation energy of  $V_O$  is sample-dependent but, at a few eV [16], suggests that annealing in vacuo at higher temperatures and for much longer times than those used in the current study would be required to produce significant concentrations of  $V_O$  in the films [17]. This provides

an explanation for the null results in the present measurements for the vacuum-annealed samples.

We have previously attributed an increase in  $S$  to an increase in oxygen vacancies in TiO<sub>2</sub> films [4]. It is unwise to place too much credibility on the film positron diffusion length values thrown up by VEPFIT (they do not vary much - between 12 and 20nm), so we shall instead use the values of  $S$  to estimate oxygen vacancy concentrations. We need first to accept the value for bulk crystalline TiO<sub>2</sub> we previously measured - 0.8285, and the defect  $S$  value of 0.895 we derived in Ref. 3, a value which is consistent with the very low diffusion lengths we measure in the films. Then the defect concentration per atom,  $C_D$ , is given by

$$(S-S_B)\lambda/(S_D-S)v \quad (1)$$

where  $S$  is the fitted film parameter,  $S_B$  is the bulk value (0.8285),  $S_D$  is the defect parameter (0.895),  $\lambda$  is the positron decay rate in undefected TiO<sub>2</sub> ( $6.76 \times 10^9 \text{ s}^{-1}$ ) and  $v$  is the specific trapping rate for the defect, which we assumed previously to be  $10^{15} \text{ s}^{-1}$ .

Thus we obtain

$$C_D = 6.8(S - 0.8285)/(0.895 - S) \times 10^{-6} \text{ per atom} \quad (2)$$

and, assuming an atomic number density of  $3 \times 10^{22} \text{ cm}^{-3}$ ,

$$C_D = 2(S - 0.8285)/(0.895 - S) \times 10^{17} \text{ cm}^{-3} \quad (3)$$

This gives *semi-quantitative* values for  $C_D$  for the 100, 150 and 220nm films of 3, 5 and 9  $\times 10^{17} \text{ cm}^{-3}$  (as-grown/vacuum-annealed) and 5, 2 and 2  $\times 10^{18} \text{ cm}^{-3}$  (H<sub>2</sub>-annealed). The uncertainties in the absolute values of these numbers may be as high as 50%, but they give an indication of the relative changes seen.



## 5. Conclusions

VEPAS studies of TiO<sub>2</sub> films grown on p<sup>+</sup>Si substrates indicate the presence of oxygen vacancies V<sub>O</sub> at concentrations C<sub>D</sub> between 10<sup>17</sup> and 10<sup>18</sup> cm<sup>-3</sup> in as-grown films, with C<sub>D</sub> increasing with film thickness from 100 to 220 nm. No significant change in C<sub>D</sub> is observed after annealing at 500°C in vacuum, but after annealing at 500°C in a hydrogen ambient C<sub>D</sub> increases by over an order of magnitude for the 100 nm film, by a factor of ~ 4 for the 150 nm film, and marginally for the 220 nm film. These conclusions are largely, but not totally, in agreement with a model which links V<sub>O</sub> concentration with EL efficiency; preliminary measurements of the latter show an increase with film thickness and after annealing in vacuum or hydrogen. The enhancement of V<sub>O</sub> concentrations in TiO<sub>2</sub>/p<sup>+</sup>Si heterostructures by appropriate plasma or annealing treatments thus appears to hold promise for the development of efficient solid state devices in silicon-based opto-electronics, and further work in this area is warranted.

## Acknowledgement

This work was partially supported by Zhejiang Provincial Natural Science Fund (No. R4090055) and "973 project" (No. 2007CB613403).

## References

- [1] T.L. Thompson, J.T. Yates Jr, Chem. Rev. **106** (2006) 4428-4453.
- [2] X. Kong, C. Liu, W. Dong, X. Zhang, C. Tao, L. Shen, J. Zhou, Y. Fei, S. Ruan S, Appl. Phys. Lett. **94** (2009) 123502:1-3.
- [3] Y.Y. Zhang, X.Y. Ma, P.L. Chen, D.S. Li, D.R. Yang, Appl. Phys. Lett. **94** (2009) 061115:1-3.
- [4] Y.Y. Zhang, X.Y. Ma, P.L. Chen, D.S. Li, X.D. Pi, D.R. Yang, P.G. Coleman, Appl. Phys. Lett. **95** (2009) 252102:1-3.
- [5] A. van Veen, H. Schut, P.E. Mijnders, in: P. G. Coleman (Ed.), Positron Beams, Their Applications, World Scientific, Singapore, 2000, pp. 191-225.
- [6] A. van Veen, H. Schut, J.de Vries, R.A. Hakvoort, M. R. Ijpma, AIP Conf. Proc. **218** (1990) 171-198.
- [7] R. Mahapatra, N. Poolamai, S. Chattopadhyay, N.G. Wright, A.K. Chakroborty, K.S. Coleman, P.G. Coleman, C.P. Burrows, Appl. Phys. Lett. **88** (2006) 072910:1-3.
- [8] J. Dekker, K. Saarinen, H. Ólafsson, E. O. Sveinbjörnsson, Appl. Phys. Lett. **82** (2003) 2020-2022.
- [9] M. Maekawa, A. Kawasuso, M. Yoshikawa, A. Miyashita, R. Suzuki, T. Ohdaira, Phys. Rev. B **73** (2006) 014111 :1-9.
- [10] U. Myler, P. J. Simpson, Phys. Rev. B **56** (1997) 14303-14309.
- [11] J.A. Baker, P.G. Coleman, N.B. Chilton, Vacuum **41** (1990) 1593-1594.
- [12] S. Szpala, P. Asoka-Kumar, B. Nielsen, J.P. Peng, S. Hayakawa, K.G. Lynn, H.-J. Gossmann, Phys. Rev. B **54** (1996) 4722-4731.
- [13] M. K. Nowotny, T. Bak, J. Nowotny and C. C. Sorrell, Phys. Stat. Sol. B **242** (2005) R88-90.

- [14] Gongming Wang et al., Nano Letts. **11** (2011) 3026-3033.
- [15] Lifeng Liu, Jinfeng Kang, Yi Wang, Xing Zhang and Ruqi Han, Jpn. J. Appl. Phys. **47** (2008) 8787-8789.
- [16] A. Janotti, J. B. Varley, P. Rinke, N. Umezawa, G. Kresse and C. G. Van de Walle, Phys. Rev. B **81** (2010) 085212-1-7.
- [17] Koji Iijima et al., J. Luminescence **128** (2008) 911–913.

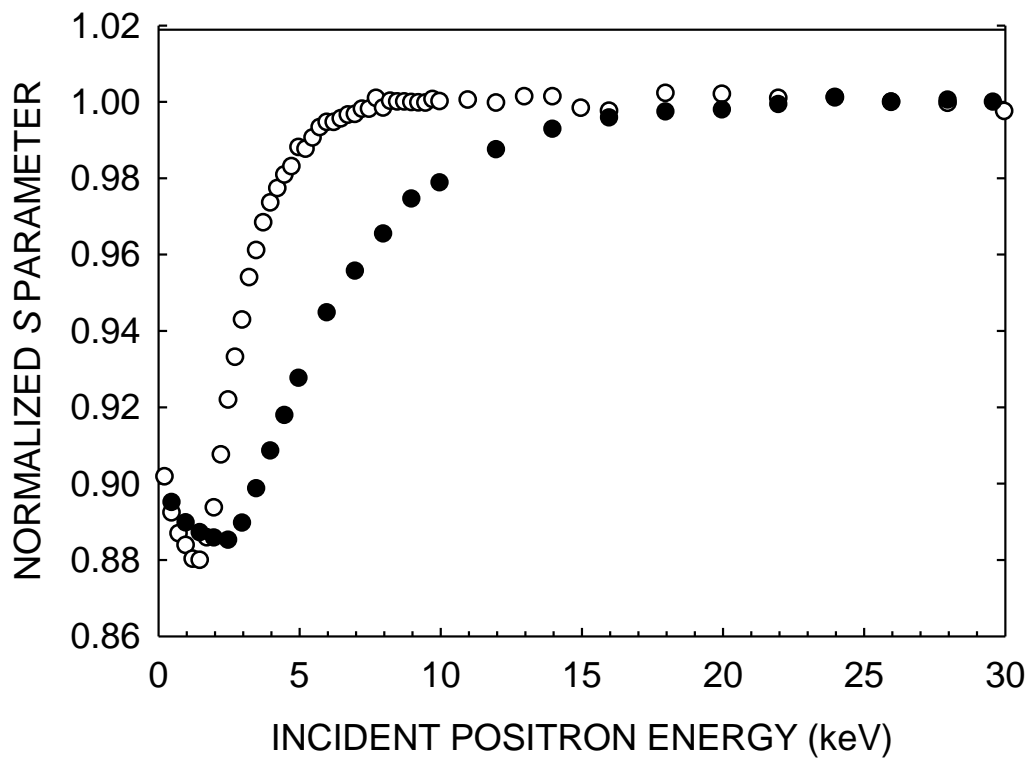


**Figure 1**

Normalized  $S(E)$  for 100 nm-thick films on Si substrates. Open circles: current  $\text{TiO}_2/\text{p}^+\text{Si}$  structure: solid circles:  $\text{TiO}_2$  film on a different Si substrate.

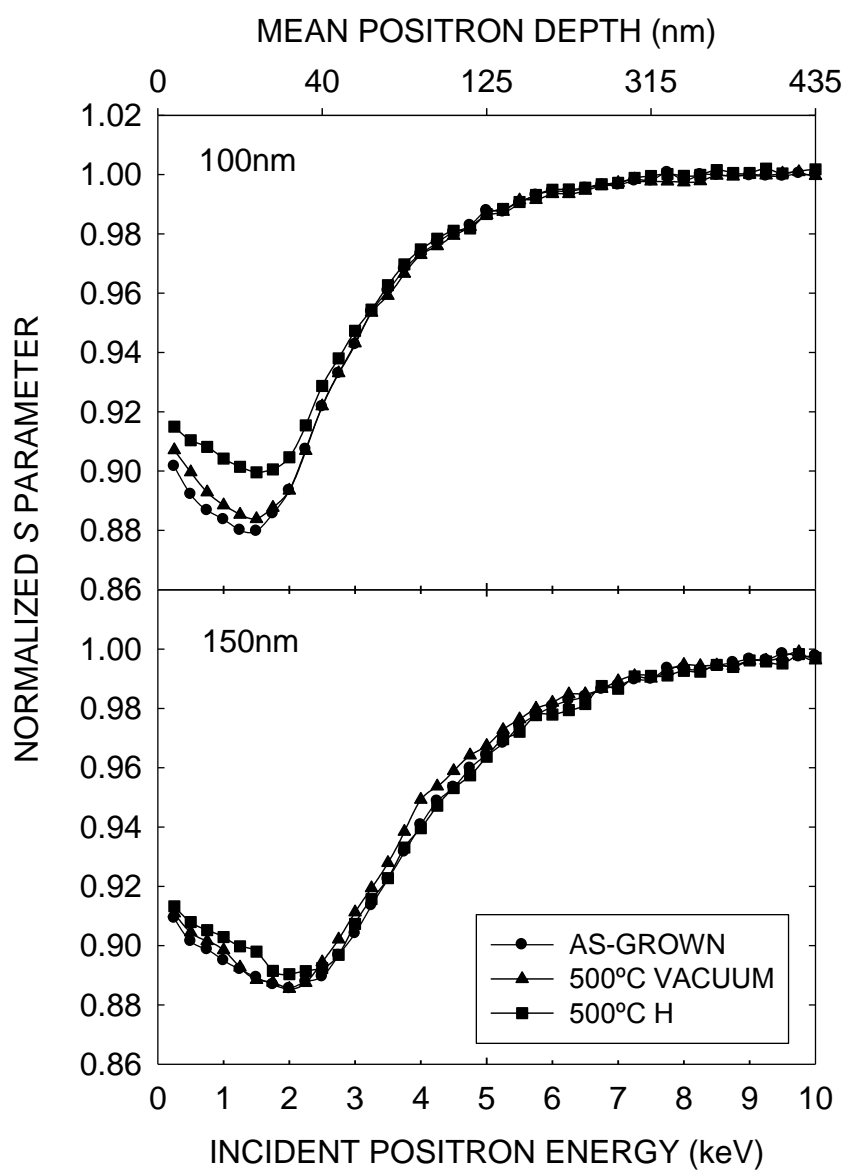


**Figure 2**

Normalized  $S(E)$  for 100 nm and 150 nm-thick films on  $\text{p}^+\text{Si}$  substrates, as-grown and after annealing at 500 °C for 1 h in vacuum and in hydrogen.

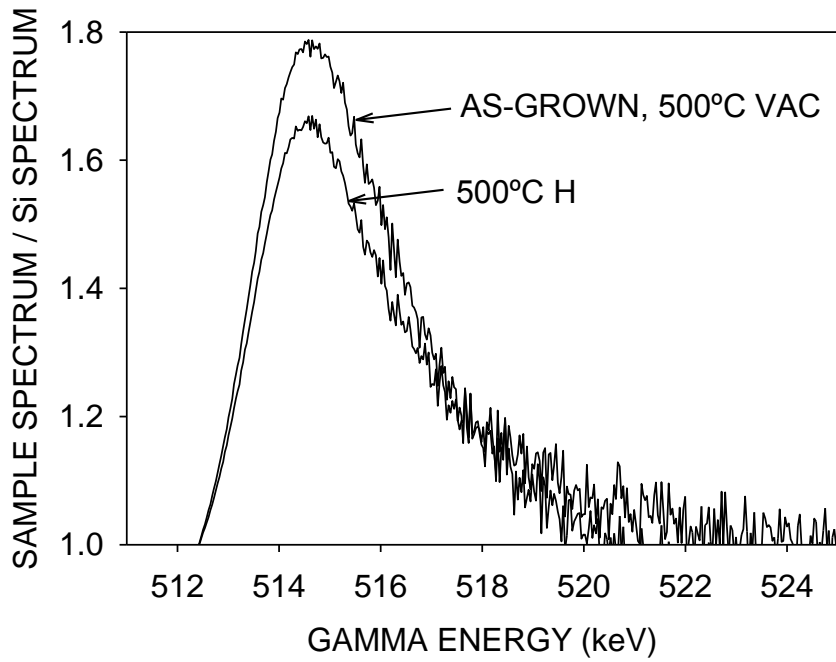


**Figure 3**

Ratio of annihilation line spectrum for 100 nm-thick  $\text{TiO}_2/\text{p}^+\text{Si}$  sample at 1.5 keV to that for defect-free silicon; total counts in both spectra are the same. The vertical line indicates the mean energy associated with annihilation by oxygen electrons.

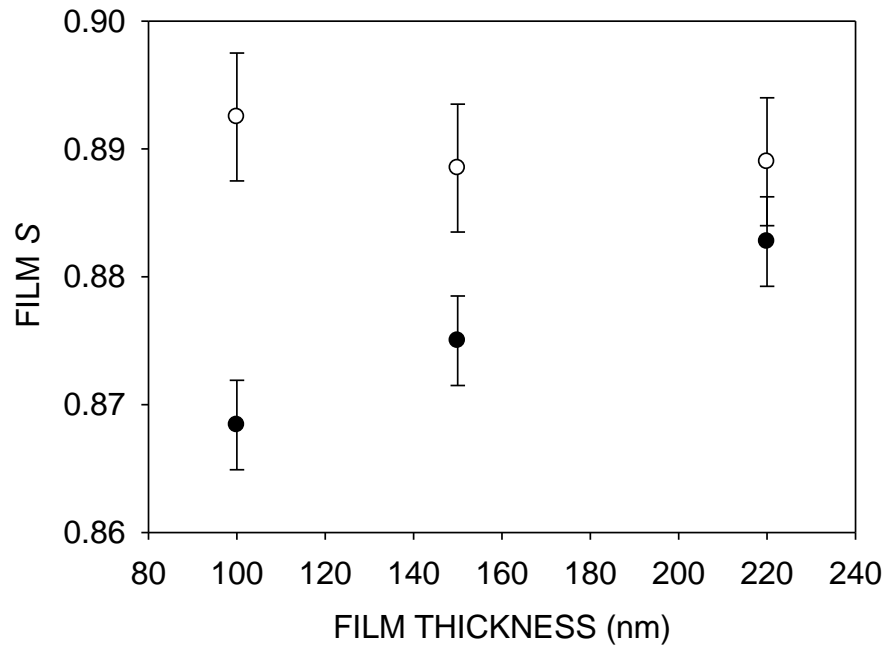


**Figure 4**

Fitted film  $S$  values for each film thickness. Black circles - average of as-grown and vacuum annealed samples; white circles – H<sub>2</sub>-annealed samples.